

Mixed Convection Boundary-Layer Flow Along a Vertical Cylinder Embedded in a Porous Medium Filled by a Nanofluid

Azizah Mohd Rohni · Syakila Ahmad ·
John H. Merkin · Ioan Pop

Received: 11 April 2012 / Accepted: 4 October 2012 / Published online: 24 October 2012
© Springer Science+Business Media Dordrecht 2012

Abstract The steady mixed convection boundary-layer flow on a vertical circular cylinder embedded in a porous medium filled by a nanofluid is studied for both cases of a heated and a cooled cylinder. The governing system of partial differential equations is reduced to ordinary differential equations by assuming that the surface temperature of the cylinder and the velocity of the external (inviscid) flow vary linearly with the axial distance x measured from the leading edge. Solutions of the resulting ordinary differential equations for the flow and heat transfer characteristics are evaluated numerically for various values of the governing parameters, namely the nanoparticle volume fraction ϕ , the mixed convection or buoyancy parameter λ and the curvature parameter γ . Results are presented for the specific case of copper nanoparticles. A critical value λ_c of λ with $\lambda_c < 0$ is found, with the values of $|\lambda_c|$ increasing as the curvature parameter γ or nanoparticle volume fraction ϕ is increased. Dual solutions are seen for all values of $\lambda > \lambda_c$ for both aiding, $\lambda > 0$ and opposing, $\lambda < 0$, flows. Asymptotic solutions are also determined for both the free convection limit ($\lambda \gg 1$) and for large curvature parameter ($\gamma \gg 1$).

Keywords Dual solutions · Mixed convection · Nanofluid · Porous medium · Vertical cylinder

A. M. Rohni
School of Quantitative Sciences, Universiti Utara Malaysia, 06010 Sintok, Kedah, Malaysia

S. Ahmad
School of Mathematical Sciences, Universiti Sains Malaysia, 11800 USM, Penang, Malaysia

J. H. Merkin
Department of Applied Mathematics, University of Leeds, Leeds, LS2 9JT, UK

I. Pop (✉)
Department of Mathematics, Babeş-Bolyai University, 400084 Cluj-Napoca, Romania
e-mail: popm.ioan@yahoo.co.uk

1 Introduction

A nanofluid is a two-phase mixture in which the solid phase consists of nanosized particles. Since the size of the particles is less than 100 nm, nanofluids behave much more like a fluid than a mixture (Xuan and Roetzel 2000; Maliga et al. 2005). Xuan and Roetzel (2000) proposed a homogeneous flow model where the convective transport equations of pure fluids are directly extended to nanofluids. This means that all the traditional heat transfer correlations can be used for nanofluids provided the properties of pure fluids are replaced by those of nanofluids involving the volume fraction of the nanoparticles (Kumar et al. 2010). These homogeneous flow models are, however, in conflict with the experimental observations of Maliga et al. (2005) who considered forced convection flow case, as they under predict the heat transfer coefficients of nanofluids. The basic flow in a nanofluid involves the effects of gravity, Brownian force and the friction force between the fluid and the ultrafine particles, the phenomena of Brownian diffusion, sedimentation and dispersion. Thus, although the nanoparticles are ultrafine, the slip between the fluid and the particles may not be zero.

Choi (1995) was the first to introduce the term nanofluid to represent a fluid in which nano-scale particles are suspended in a base fluid with a low thermal conductivity such as water, ethylene glycol, oils, etc. In recent years, the concept of a nanofluid has been proposed as a route for enhancing the performance of the heat transfer rates in the liquids that are currently used. Materials with sizes of nanometers possess unique physical and chemical properties (Das et al. 2007). They can flow smoothly through microchannels without clogging because they are sufficiently small to behave similar to liquid molecules (Khanafer et al. 2003). This fact has attracted much research into the investigation of the heat transfer characteristics in nanofluids. It has been found that the presence of nanoparticles within the fluid can appreciably increase the effective thermal conductivity of the fluid and, as a consequence, enhance the heat transfer characteristics. An excellent collection of articles on this topic can be found in the book by Das et al. (2007) and in the review papers by Buongiorno (2006), Trisaksri and Wongwises (2007), Kakaç and Pramuanjaroenkij (2009), Lee et al. (2010), Eagen et al. (2010), Wong and Leon (2010), Fan and Wang (2011), Sheikholeslami et al. (2012a,b) and Soleimani et al. (2012).

Here we study the steady, mixed convection boundary-layer flow along a vertical circular cylinder embedded in a porous medium filled with a nanofluid for the cases of both a heated and a cooled cylinder. We apply the mathematical nanofluid model proposed by Tiwari and Das (2007) in combination with Darcy's law for the flow in the porous medium and the Boussinesq approximation for the convective forces. For our numerical calculations we take the specific case of copper nanoparticles, though we expect the nature of our results to be more widely applicable to other forms of similar types of nanoparticles. We take an outer flow and wall temperature distribution that enables the problem to be reduced to similarity form with the resulting similarity equations then being discussed in detail. Convective flow within porous media both with or without nanoparticles have a wide range of practical and engineering applications see, for example the books by Nield and Bejan (2006), Ingham and Pop (2005), Pop and Ingham (2001), Vafai (2005, 2010) and Vadasz (2008).

In a series of pioneering papers, Kuznetsov and Nield (2010a,b,c, 2011a,b,c) and Nield and Kuznetsov (2009a,b, 2011) have used the mathematical nanofluid model proposed by Buongiorno (2006) to study some problems on viscous (regular) fluids and porous media filled by nanofluids. The authors have assumed that nanoparticles are suspended in the nanofluid using either surfactant or surface charge technology. This prevents particles from agglomeration and deposition on the porous matrix. On the other hand, it is very important to explain how nanofluid flow is possible in a porous medium. Thus, one of the anonymous Reviewer

of this paper has pointed out that without special precautions, nanoparticles will be simply absorbed by the porous matrix. Basically, the porous matrix will work as a filter for nanoparticles. This situation has been described, explained, and modelled in the recent papers by [Wu et al. \(2010, 2011\)](#). The physical situation described in these papers show that the work on porous media filled by nanofluids are not just a mathematical exercise, but are based on deep physical understanding of nanofluid flows. This demonstrates that we are simulating here a real physics problem of mixed convection flow and heat transfer in a porous medium filled by a nanofluid.

2 Mathematical Model

We consider the steady, axisymmetric boundary-layer flow along a vertical cylinder of radius a which is embedded in a porous medium filled with a nanofluid. It is assumed that the velocity of the outer (potential) flow $u_e(x)$ and the surface temperature $T_w(x)$ are of the form $u_e(x) = U_0x/a$ and $T_w(x) = T_\infty + T_0x/a$, where U_0 and T_0 are constants with $U_0 > 0$ and $T_0 > 0$ for a heated cylinder (assisting flow), $T_0 < 0$ for a cooled cylinder (opposing flow), respectively. Under these assumptions along with the Boussinesq and boundary-layer approximations, and using the nanofluid model proposed by [Tiwari and Das \(2007\)](#), the basic equations are

$$\frac{\partial(ru)}{\partial x} + \frac{\partial(rv)}{\partial r} = 0 \tag{1}$$

$$\frac{\mu_{nf}}{\mu_f} \frac{\partial u}{\partial r} = \frac{gK [(1 - \phi)\rho_f\beta_f + \phi\rho_s\beta_s]}{\mu_f} \frac{\partial T}{\partial r} \tag{2}$$

$$u \frac{\partial T}{\partial x} + v \frac{\partial T}{\partial r} = \frac{\alpha_{nf}}{r} \frac{\partial}{\partial r} \left(r \frac{\partial T}{\partial r} \right) \tag{3}$$

subject to the boundary conditions

$$v = 0, \quad T = T_\infty + T_0 \frac{x}{a} \text{ on } r = a, \quad u \rightarrow U_0 \frac{x}{a}, \quad T \rightarrow T_\infty \text{ as } r \rightarrow \infty \tag{4}$$

Here x and r are the cylindrical coordinates measured along the axis of the cylinder and normal to the surface of the cylinder in the radial direction, u and v are the velocity components in the x and r directions, respectively, and T is the temperature of the nanofluid. g is the acceleration due to gravity, ϕ is the nanoparticle volume fraction, β_f and β_s are the coefficients of thermal expansion of the fluid and of the solid, respectively, ρ_f and ρ_s are the densities of the fluid and of the solid fractions, respectively, μ_{nf} is the viscosity and α_{nf} is the thermal diffusivity of the nanofluid. These are given by [Khanafer et al. \(2003\)](#) and [Oztop and Abu-Nada \(2008\)](#), for example, as

$$\mu_{nf} = \frac{\mu_f}{(1 - \phi)^{2.5}}, \quad \alpha_{nf} = \frac{k_{nf}}{(\rho C_p)_{nf}}, \quad (\rho C_p)_{nf} = (1 - \phi)(\rho C_p)_f + \phi(\rho C_p)_s \tag{5}$$

$$\frac{k_{nf}}{k_f} = \frac{(k_s + 2k_f) - 2\phi(k_f - k_s)}{(k_s + 2k_f) + \phi(k_f - k_s)}$$

where μ_f is the dynamic viscosity of the base fluid with an expression for it being proposed by [Brinkman \(1952\)](#), k_{nf} is the thermal conductivity of the nanofluid, k_f and k_s are the thermal conductivities of the base fluid and of the solid, respectively, and $\rho(C_p)_{nf}$ is the heat capacitance of the nanofluid. Strictly expressions (5) are restricted to spherical (or near spherical) nanoparticles with other expressions being required for other shapes of nanoparticles.

Equations (1–3) with the boundary conditions (4) can be transformed into ordinary differential equations by the similarity transformation, see Mahmood and Merkin (1988) and Merkin and Pop (1987), for example,

$$\eta = \frac{r^2 - a^2}{2\alpha_f a} \left(\frac{U_0 \alpha_f}{2a} \right)^{1/2}, \quad \psi = (2U_0 a \alpha_f)^{1/2} x f(\eta), \quad \theta(\eta) = \frac{T - T_\infty}{T_w - T_\infty} \tag{6}$$

where ψ is the stream function defined as $u = r^{-1} \partial \psi / \partial r$ and $v = -r^{-1} \partial \psi / \partial x$. Using (6) Eqs. (2,3) reduce to the ordinary differential equations

$$f'' = B(\phi) \lambda \theta' \tag{7}$$

$$A(\phi) [(1 + 2\gamma\eta)\theta'' + 2\gamma\theta'] + 2f\theta' - 2f'\theta = 0 \tag{8}$$

subject to the boundary conditions

$$f(0) = 0, \quad \theta(0) = 1, \quad f'(\eta) \rightarrow 1, \quad \theta(\eta) \rightarrow 0 \quad \text{as } \eta \rightarrow \infty \tag{9}$$

where prime denotes differentiation with respect to η . The parameters A and B are given by

$$A = A(\phi) = \frac{k_{nf}/k_f}{(1 - \phi) + \phi(\rho C_p)_s/(\rho C_p)_f}$$

$$B = B(\phi) = (1 - \phi)^{2.5} \left[(1 - \phi) + \phi \left(\frac{\rho_s \beta_s}{\rho_f \beta_f} \right) \right] \tag{10}$$

and for a given nanofluid and porous material, the parameters A and B depend only on ϕ , the nanoparticle volume fraction. When $\phi = 0$ (regular fluid), $A = B = 1$ and, as the nanoparticle volume fraction ϕ increases, A increases and B decreases, with $B \rightarrow 0$ as $\phi \rightarrow 1$. The constants γ and λ are, respectively, the curvature and the buoyancy parameters defined by

$$\gamma = \left(\frac{2\alpha_f}{U_0 a} \right)^{1/2}, \quad \lambda = \frac{Ra}{Pe} \tag{11}$$

where $Ra = gK\beta_f T_0/(\alpha_f \nu_f)$ and $Pe = U_0 a/\alpha_f$ are the Rayleigh number and the Péclet number for the porous medium, respectively.

Integrating Eq. (7) and applying boundary conditions (9) gives

$$f' = B\lambda\theta + 1 \tag{12}$$

where $B(\phi)$ is defined in (10). Expression (12) shows that the dimensionless vertical velocity depends linearly on the temperature. Further, if we combine Eqs. (8) and (12), we obtain

$$A [(1 + 2\gamma\eta)f'''' + 2\gamma f'''] + 2f f'' - 2f'^2 + 2f' = 0 \tag{13}$$

on $0 \leq \eta < \infty$. The boundary conditions are now

$$f(0) = 0, \quad f'(0) = B\lambda + 1, \quad f'(\eta) \rightarrow 1 \quad \text{as } \eta \rightarrow \infty \tag{14}$$

Having $\lambda > 0$ corresponds to an assisting (or aiding) flow, $\lambda < 0$ corresponds to an opposing flow. For $\lambda = 0$, Eqs. (7) and (8) are decoupled and this case corresponds to the forced convection flow past the vertical cylinder. Further, $\phi = 0$ corresponds to a regular fluid and $\gamma = 0$ to a flat plate. In this case, Eqs. (13) and (14) reduce to those for the problem of steady mixed convection boundary-layer flow along a vertical flat plate embedded in a porous medium considered by Aly et al. (2003) when $\lambda = 1$ in their notation for the variable wall temperature. We notice also that, if $\phi = 0$ and $\gamma = 0$, the problem reduces to that studied by Merkin (1980, 1985).

Table 1 Values of the parameters $A(\phi)$ and $B(\phi)$ defined in (10) using the thermophysical properties of water and copper Cu taken from Oztop and Abu-Nada (2008)

| ϕ | $A(\phi)$ | $B(\phi)$ |
|--------|-----------|-----------|
| 0.05 | 1.1673 | 0.8670 |
| 0.1 | 1.3553 | 0.7463 |
| 0.2 | 1.8089 | 0.5395 |

The physical quantities of interest are the skin friction coefficient C_f and the local Nusselt number Nu_x , which are defined as

$$C_f = \frac{\tau_w}{\rho_f u_e^2}, \quad Nu_x = \frac{xq_w}{k_f(T_w - T_\infty)} \tag{15}$$

where the skin friction τ_w and heat transfer from the plate q_w are given by

$$\tau_w = \mu_{nf} \left(\frac{\partial u}{\partial r} \right)_{r=a}, \quad q_w = -k_{nf} \left(\frac{\partial T}{\partial r} \right)_{r=a} \tag{16}$$

Using the similarity variables (6), we have

$$(2Pe_x^{1/2}/Pr)C_f = \frac{1}{(1-\varphi)^{2.5}} f''(0), \quad (2/Pe_x)^{1/2} Nu_x = -\frac{k_{nf}}{k_f} \theta'(0) \tag{17}$$

where $Pe_x = u_e(x)x/\alpha_f$ is the local Péclet number and $Pr = V_f/\alpha_f$ is the Prandtl number of the porous medium.

We start by considering the numerical solutions to Eqs. (13, 14).

3 Numerical Results

Here we discuss the numerical solution to Eq. (13) subject to boundary conditions (14) for selected values of the parameters, our main objectives being to assess the effects that curvature and the nanoparticles have on the convective flow and heat transfer. We use the data for Cu nanoparticles in water provided by Oztop and Abu-Nada (2008) with the resulting values for A and B , defined in (10), for different volume fractions ϕ being given in Table 1.

We start by considering the case of a pure fluid, $\phi = 0$. In Fig. 1a we plot $f''(0)$ against the mixed convection parameter λ for different values of the curvature parameter γ . We see that there is a critical value λ_c of λ , with the values of $|\lambda_c|$ increasing with γ . There is a saddle-node bifurcation at $\lambda = \lambda_c$ giving rise to two solution branches for $\lambda > \lambda_c$. Both solution branches continue into the aiding flow, $\lambda > 0$, region with the upper solution branch passing through the forced convection solution $f = \eta$ at $\lambda = 0$. On this branch $f''(0) > 0$ for opposing flow, $\lambda_c \leq \lambda < 0$ and $f''(0) < 0$ for aiding flow, $\lambda > 0$. The numerical solutions for the lower solution branch (shown by a broken line) also pass smoothly through $\lambda = 0$ without a singularity appearing, as seen for example in Merkin (1980). Even though a solution to (13,14) exists on the lower branch when $\lambda = 0$, it cannot be a physically acceptable solution to our original problem where the temperature is related to the velocity via expression (12). This can be seen in Fig. 1b where we plot the corresponding values of $-\theta'(0)$ with $\theta'(0)$ being calculated from (12) as $\theta'(0) = f''(0)/B\lambda$ clearly showing the discontinuity seen in the figure as $|\lambda| \rightarrow 0$. We expect, through the saddle-node bifurcation, that these lower branch solutions to be unstable.

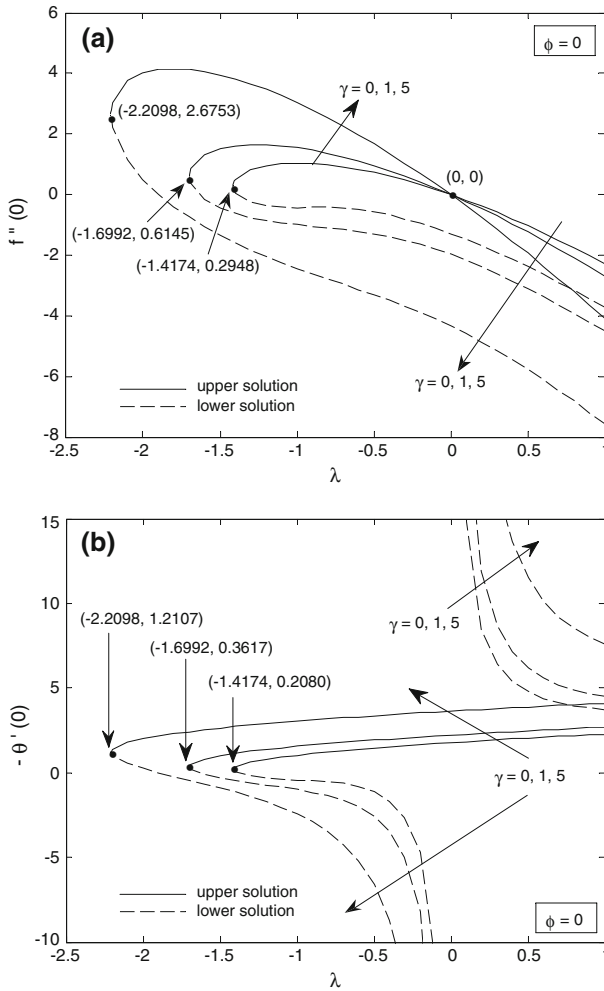


Fig. 1 Plots of **a** the skin friction $f''(0)$, **b** the surface heat transfer $-\theta'(0)$ against the mixed convection parameter λ for different values of curvature parameter γ when $\phi = 0$

In Figs. 2, 3, and 4 we assess the effects of both curvature and the addition of nanoparticles on the convective flow by plotting $f''(0)$ and $-\theta'(0)$ against λ . In Fig. 2 we take $\gamma = 0$, giving a flat surface, and nanoparticle volume fractions of $\phi = 0$ (pure fluid), $\phi = 0.05$, $\phi = 0.1$ and $\phi = 0.2$ with the corresponding values of the parameters A and B appearing in Eqs. (13,14) given in Table 1. In Fig. 2 we see that the effect of adding nanoparticles to the base fluid is to increase the range of existence of solutions in the opposing flow region and to decrease the friction effects on the surface, Fig. 2a, positive for opposing flow and negative for aiding flow. The addition of nanoparticles also increases the surface heat flux, Fig. 2b, on the upper solution branch.

These features are also seen when the curvature is increased to $\gamma = 1$ in Fig. 3 and more noticeably to $\gamma = 5$ in Fig. 4. For each nanoparticle volume fraction ϕ the effect of curvature γ is to increase the range of existence of solutions and to increase both the skin friction

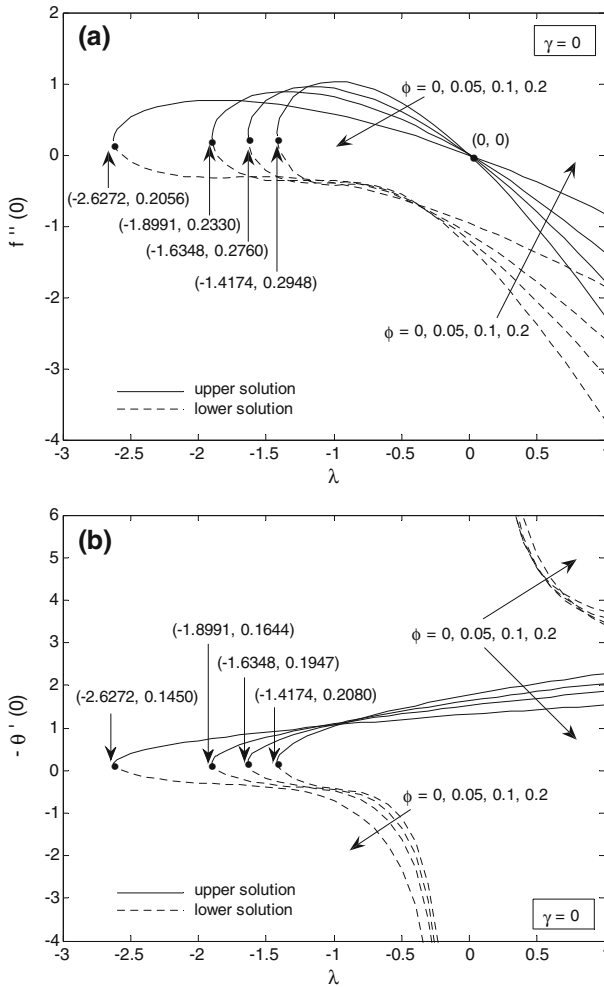


Fig. 2 Plots of **a** the skin friction $f''(0)$, **b** the surface heat transfer $-\theta'(0)$ against the mixed convection parameter λ for the addition of copper (Cu) nanoparticles with volume fractions $\phi = 0.0, 0.05, 0.1, 0.2$ for $\gamma = 0$ (flat surface)

and surface heat transfer, consistent with Fig. 1. For a given curvature the effect of adding nanoparticles is again to increase the range of solutions for opposing flow, to decrease skin friction effects and to decrease the surface heat transfer, following the trends seen for a flat surface in Fig. 2.

We have identified critical values λ_c of λ determining the range of existence of a solution for opposing flow. We have also seen the values of $|\lambda_c|$ increase with both increased curvature and with the addition of nanoparticles. We now consider these critical values in a little more detail.

3.1 Critical Values

For given values of the other parameters we calculated the critical values λ_c of (13,14) following the approach described in Merkin (1985) and Merkin and Mahmood (1989). In Fig. 5

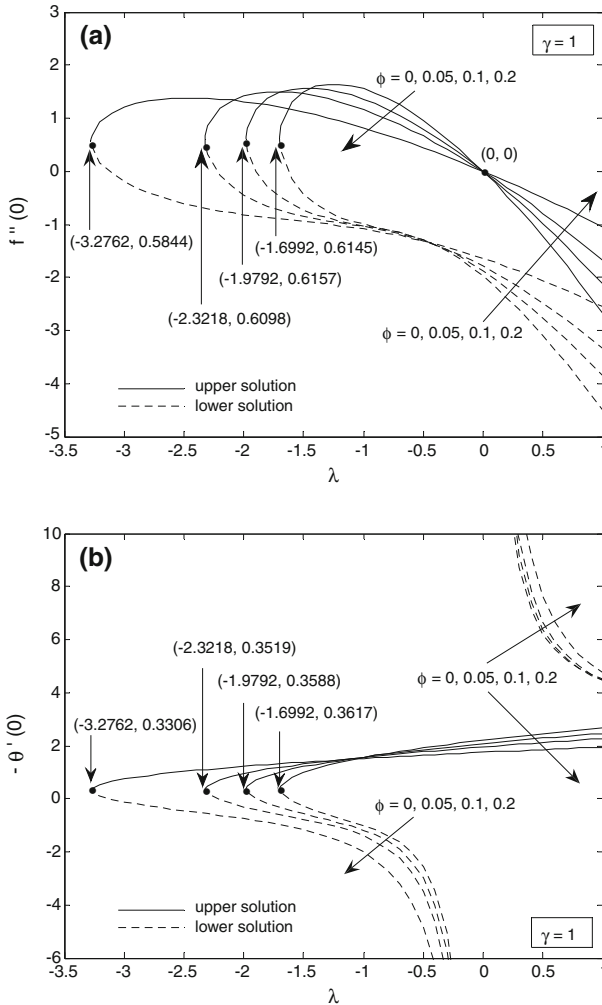


Fig. 3 Plots of **a** the skin friction $f''(0)$, **b** the surface heat transfer $-\theta'(0)$ against the mixed convection parameter λ for the addition of copper (Cu) nanoparticles with volume fractions $\phi = 0.0, 0.05, 0.1, 0.2$ for $\gamma = 1$

we plot these critical values λ_c against γ for the nanoparticle volume fractions labelled in the figure. We see that, in every case, λ_c is negative and that $|\lambda_c|$ increases as the curvature parameter γ is increased. Also the figure shows that, for a given curvature, increasing the volume fraction of the nanoparticles increases $|\lambda_c|$ and hence the range of possible solutions for opposing flow. The results in Fig. 5 are in agreement with the values shown in Figs. 1, 2, 3, and 4. Also, again consistent with Figs. 2, 3, and 4, the values of $f''(0)$ at the critical point increase with γ and appear to be insensitive to the nanoparticle volume fraction ϕ .

We now consider some limiting asymptotic forms which give further insights into the behaviour of the convective flow.

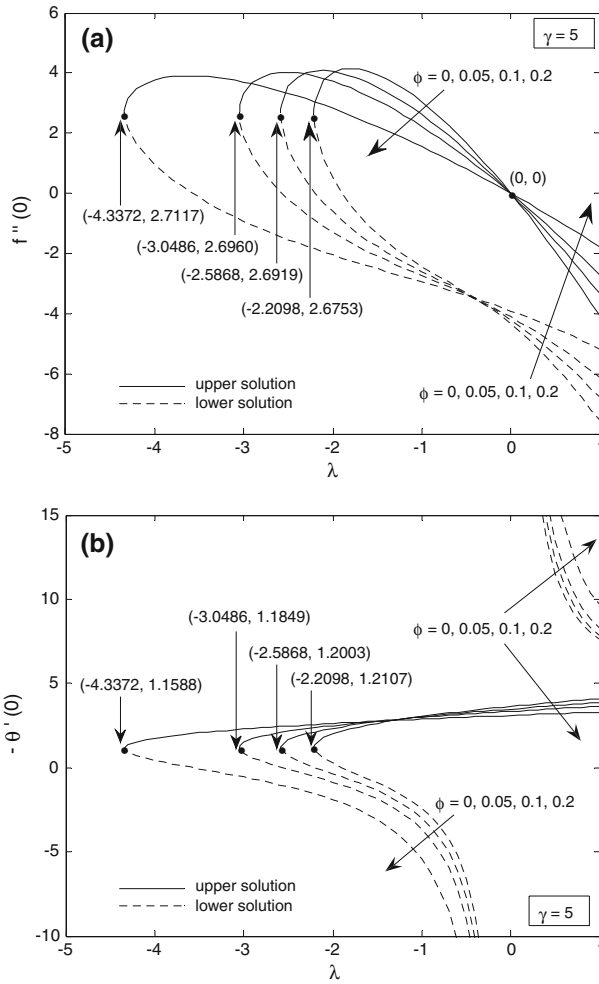


Fig. 4 Plots of **a** the skin friction $f''(0)$, **b** the surface heat transfer $-\theta'(0)$ against the mixed convection parameter λ for the addition of copper (Cu) nanoparticles with volume fractions $\phi = 0.0, 0.05, 0.1, 0.2$ for $\gamma = 5$

4 Asymptotic Limits

4.1 Free Convection Limit, λ Large

To obtain a solution to Eqs. (13, 14) for $\lambda \gg 1$ we put

$$f = \lambda^{1/2}F, \quad \zeta = \lambda^{1/2}\eta \tag{18}$$

Equation (13) then becomes

$$A \left((1 + 2\gamma\lambda^{-1/2}\zeta) F''' + 2\gamma\lambda^{-1/2}F'' \right) + 2FF'' - 2F'^2 + 2\lambda^{-1}F' = 0 \tag{19}$$

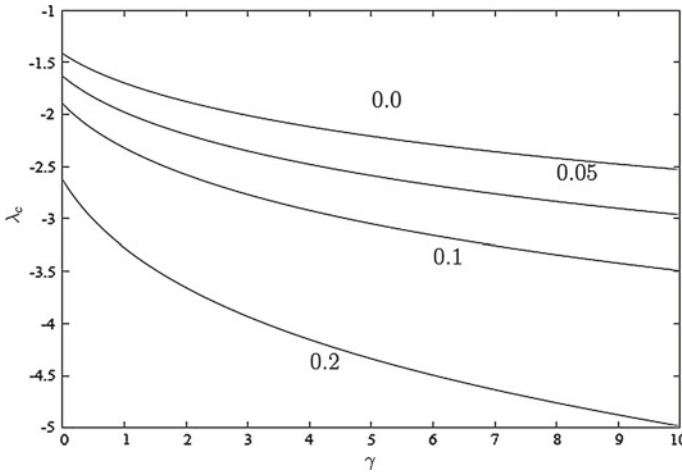


Fig. 5 The critical values λ_c of Eq. (13) subject to (14) plotted against γ for nanoparticle volume fractions $\phi = 0.0, 0.05, 0.1, 0.2$

where primes now denote differentiation with respect to ζ , subject to the boundary conditions

$$F(0) = 0, \quad F'(0) = B + \lambda^{-1}, \quad F' \rightarrow \lambda^{-1} \quad \text{as } \zeta \rightarrow \infty \tag{20}$$

The leading-order problem is then, for γ of $O(1)$,

$$AF_0''' + 2F_0F_0'' - 2F_0'^2 = 0, \quad F_0(0) = 0, \quad F_0'(0) = B, \quad F_0' \rightarrow 0 \quad \text{as } \zeta \rightarrow \infty \tag{21}$$

Equation (21) has the solution

$$F_0(\zeta) = \sqrt{\frac{AB}{2}} \left(1 - e^{\sqrt{2B/A}\zeta}\right) \tag{22}$$

giving

$$\left(\frac{d^2 f}{d\eta^2}\right)_{\eta=0} \sim -\frac{B\sqrt{2B}}{\sqrt{A}}\lambda^{3/2} + \dots, \quad \left(\frac{d\theta}{d\eta}\right)_{\eta=0} \sim -\frac{\sqrt{2B}}{\sqrt{A}}\lambda^{1/2} + \dots \quad \text{as } \lambda \rightarrow \infty \tag{23}$$

Expression (23) shows that the effect of increasing the nanoparticle volume fraction is to decrease both the skin friction and the surface heat transfer.

4.2 A Special Exact Solution

The recent papers by Magyari (2011a,b,c) and Pop (2011) on the scaling equivalence of the homogeneous nanofluid models to the corresponding regular fluid model, a special exact solution of the present flow and heat transfer problem (7)–(9) can be obtained following the solution for the regular fluid case, $A = B = 1$, given by Magyari et al. (2003). This exact solution is

$$f(\eta) = \eta + \frac{B\lambda}{c} (1 - e^{-c\eta}), \quad \theta(\eta) = e^{-c\eta} \tag{24}$$

where we require $c > 0$ and that

$$c = \sqrt{\frac{2(2 + B\lambda)}{A}}, \quad \gamma = \frac{1}{\sqrt{2A(2 + B\lambda)}} \tag{25}$$

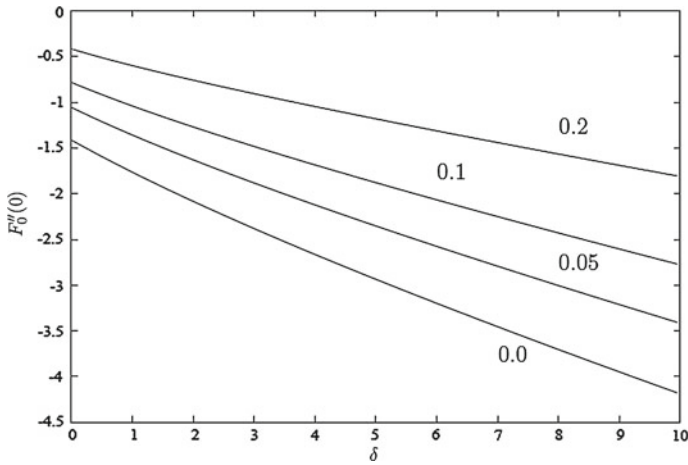


Fig. 6 The free convection limit: a plot of $F''(0)$ against the modified curvature parameter δ obtained from the numerical solution of Eq. (27) subject to the boundary conditions in (21) for nanoparticle volume fractions $\phi = 0.0, 0.05, 0.1, 0.2$

Expressions (25) require that $\gamma > 0$ and $B\lambda > -2$ putting a limit on the range of existence of this solution. The specific relationship between λ and γ given in (25), two parameters that can, in general, be varied independently, means that (24, 25) gives only a restricted class of all the solutions possible to (7)–(9), or equivalently (13, 14). From the solution given by (24,25) we have

$$f''(0) = -B\lambda\sqrt{\frac{2(2 + B\lambda)}{A}}, \quad \theta'(0) = -\sqrt{\frac{2(2 + B\lambda)}{A}} \tag{26}$$

Expressions (26) agree with (23) in the large λ limit.

Curvature effects only have a significance in this limit when γ is large, of $O(\lambda^{1/2})$. To deal with this case we put $\gamma = \delta\lambda^{1/2}$, where δ is now of $O(1)$. In this case the leading-order problem for λ large becomes

$$A((1 + 2\delta\xi)F'''_0 + 2\delta F''_0) + 2F_0F''_0 - 2F_0'^2 = 0 \tag{27}$$

still subject to the boundary conditions in (21). In Fig. 6 we plot $F''(0)$ against the modified curvature parameter δ obtained from solving (27) numerically for representative values of the nanoparticle volume fraction ϕ . This figure shows, for each value of ϕ , that $F''_0(0)$ is negative and decreases as δ is increased, as might be expected from Figs. 2, 3, and 4. This decrease with δ appears to almost linear for the larger values of δ . Again we see that the effect of increasing the nanoparticle volume fraction ϕ is, for a given curvature, to decrease the skin friction, consistent with expression (23).

4.3 Solution for Large Curvature, $\gamma \gg 1$

Here we derive a solution to Eqs. (13, 14) valid for large γ , assuming a given nanoparticle volume fraction ϕ so that we can take the parameters A and B in (13,14) and defined in (10) as constants. We start in an inner region where we make the transformation

$$f = \frac{1}{2\gamma}g, \quad y = 2\gamma\eta \tag{28}$$

Equations (13, 14) become

$$A[(1 + y)g''' + g''] + \frac{1}{2\gamma^2}(gg'' - g'^2 + g') = 0, \quad g(0) = 0, \quad g'(0) = 1 + B\lambda \quad (29)$$

where primes now denote differentiation with respect to y and the outer boundary condition is relaxed at this stage. In order to match with the outer solution we have to look for a solution to (29) by expanding in the form

$$g(y; \gamma) = g_0(y) + \frac{g_1(y)}{\log \gamma} + \frac{g_2(y)}{(\log \gamma)^2} + \dots \quad (30)$$

Solving the resulting equations so as to satisfy the boundary conditions on $y = 0$ gives

$$g_0 = (1 + B\lambda)y, \quad g_1 = a_1[(1 + y) \log(1 + y) - y], \quad g_2 = a_2[(1 + y) \log(1 + y) - y] \quad (31)$$

for constants a_1, a_2 to be determined.

An outer region is also required in which we put

$$f = \gamma G, \quad Y = \frac{\eta}{\gamma} = \frac{y}{2\gamma^2} \quad (32)$$

Equation (13) now becomes

$$A \left(Y + \frac{1}{2\gamma^2} \right) G''' + AG'' + GG'' - G'^2 + G' = 0 \quad (33)$$

subject to $G' \rightarrow 1$ as $Y \rightarrow \infty$ and, on matching with the inner region given by (30, 31),

$$G \sim (1 + B\lambda + 2a_1)Y + \frac{Y [a_1(\log(2Y) - 1) + 2a_2]}{\log \gamma} + \dots \text{ as } Y \rightarrow 0 \quad (34)$$

where primes now denote differentiation with respect to Y . Expression (34) indicates an expansion in the outer region of

$$G(Y; \gamma) = G_0(Y) + \frac{G_1(Y)}{\log \gamma} + \dots \quad (35)$$

At leading order we have

$$A [Y G_0''' + G_0''] + G_0 G_0'' - G_0'^2 + G_0' = 0 \quad (36)$$

The solution to Eq. (36) which satisfies the outer boundary condition is simply $G_0 = Y$. Matching with the inner region then gives

$$(1 + B\lambda + 2a_1) = 1 \quad \text{or} \quad a_1 = -\frac{B\lambda}{2} \quad (37)$$

At $O((\log \gamma)^{-1})$ we then have

$$AYG_1''' + (A + Y)G_1'' - G_1' = 0, \quad G_1' \rightarrow 0 \quad \text{as } Y \rightarrow \infty \quad (38)$$

and, from (34,37), that

$$G_1 \sim -\frac{B\lambda}{2} Y \log Y + \left(2a_2 + \frac{B\lambda}{2} (1 - \log 2) \right) Y + \dots \text{ as } Y \rightarrow 0 \quad (39)$$

We can solve Eq. (38) subject to (39) to get

$$G'_1 = -\frac{AB\lambda}{2} \left(\frac{e^{-Y/A} \log Y}{A + Y} - (A + Y) \int_Y^\infty \frac{e^{-s/A} (3A + s) \log s}{A(A + s)^3} ds \right) \tag{40}$$

from which it follows that

$$a_2 = \frac{B\lambda}{4} (AI_\infty + \log 2) \quad \text{where} \quad I_\infty = \int_0^\infty \frac{e^{-Y/A} (3A + Y) \log Y}{(A + Y)^3} dY \tag{41}$$

In Fig. 7a we plot $f''(0)$ against the curvature parameter γ for $\lambda = 1.0$ and for representative values of the nanoparticle volume fraction ϕ . We see that $f''(0) < 0$ in all cases and that $|f''(0)|$ increases as γ is increased, with an almost linear slope for the larger values of γ . Also, for a given value of γ , the values of $|f''(0)|$ decrease as the volume fraction ϕ is increased, consistent with Figs. 2, 3, and 4. From (28, 31, 37)

$$\begin{aligned} \left(\frac{d^2 f}{d\eta^2} \right)_{\eta=0} &\sim -B\lambda \frac{\gamma}{\log \gamma} + O(\gamma(\log \gamma)^{-2}), \\ \left(\frac{d\theta}{d\eta} \right)_{\eta=0} &\sim -\frac{\gamma}{\log \gamma} + \dots \quad \text{as } \gamma \rightarrow \infty \end{aligned} \tag{42}$$

showing that, for γ large, $f''(0)$ is independent of $A(\phi)$ and that $\theta'(0)$ is independent of both A and B , i.e. independent of the addition of nanoparticles in this limit. As a check on our asymptotic analysis we plot $f''(0) \log \gamma / \gamma$ against γ in Fig. 7b still for $\lambda = 1.0$. This curve should, from (42), approach the asymptotic limit of -1 as γ increases. We see that the curve is increasing towards this limit though very slowly. This might be expected as our theory indicates that the correction to (42) is only of $O((\log \gamma)^{-1})$ and would require γ to be very much larger than the maximum value of $\gamma = 75.0$ used for Fig. 7b. We notice at this place that the original problem (13, 14) can be rescaled to remove the parameters A and B .

5 Rescaling the Problem

For a given type of nanoparticles and a given nanoparticle volume fraction ϕ , the parameters A and B are constants and can be formally removed from the problem by a rescaling of the variables. To achieve this we put

$$f = A^{1/2} \tilde{f}, \quad \tilde{\eta} = A^{-1/2} \eta \tag{43}$$

This gives

$$(1 + 2\gamma A^{1/2} \tilde{\eta}) \tilde{f}''' + 2\gamma A^{1/2} \tilde{f}'' + 2(\tilde{f} \tilde{f}'' - \tilde{f}'^2 + \tilde{f}') = 0 \tag{44}$$

where primes now denote differentiation with respect to $\tilde{\eta}$, subject to

$$\tilde{f}(0) = 0, \quad \tilde{f}'(0) = B\lambda + 1, \quad \tilde{f}' \rightarrow 1 \quad \text{as } \tilde{\eta} \rightarrow \infty \tag{45}$$

If we now put

$$\alpha = \gamma A^{1/2}, \quad \mu = B\lambda \tag{46}$$

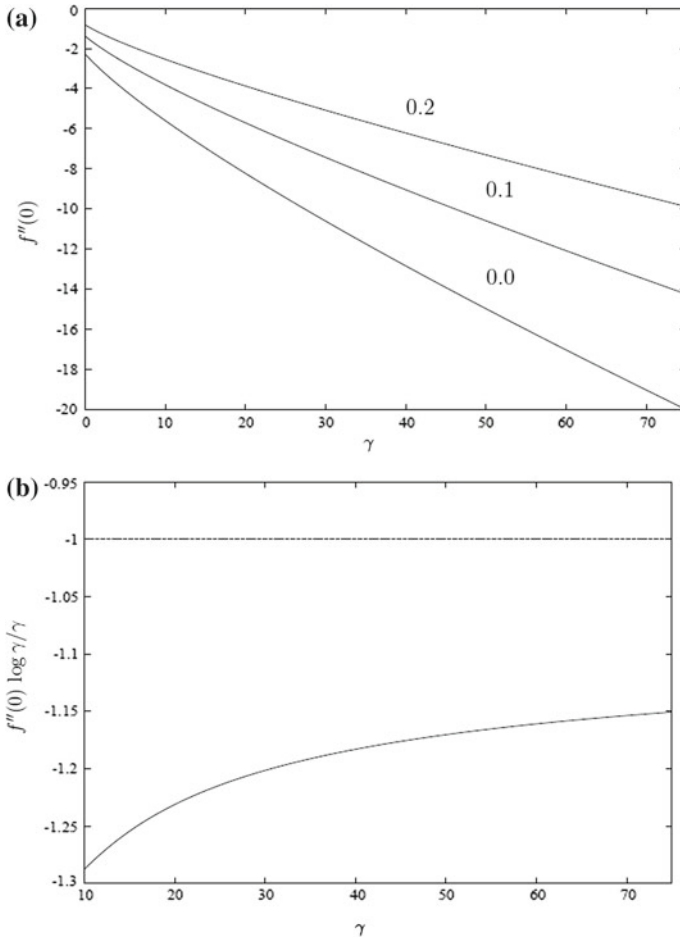


Fig. 7 Plots of **a** the skin friction $f''(0)$ against the curvature parameter γ for the mixed convection parameter $\lambda = 1.0$ and for nanoparticle volume fractions $\phi = 0.0, 0.1, 0.2$, **b** $f''(0) \log \gamma / \gamma$ against γ for $\phi = 0.0$, the asymptotic limit (42) for large γ is shown by the broken line

we obtain

$$(1 + 2\alpha\tilde{\eta})\tilde{f}''' + 2\alpha\tilde{f}'' + 2(\tilde{f}\tilde{f}'' - \tilde{f}'^2 + \tilde{f}') = 0 \tag{47}$$

where α is a modified curvature parameter and μ a modified mixed convection parameter, now subject to

$$\tilde{f}(0) = 0, \quad \tilde{f}'(0) = \mu + 1, \quad \tilde{f}' \rightarrow 1 \quad \text{as} \quad \tilde{\eta} \rightarrow \infty \tag{48}$$

This is Eq. (13) with $A = 1$ results for which are shown in Fig. 1 when γ is replaced by α . There is, for example, a critical value $\mu_c = \mu_c(\alpha)$, as plotted in Fig. 5 with $\phi = 0$. This rescaling, given by (43, 46), is consistent with the scalings for the free convection limit (18).

This rescaling is, perhaps most useful for the specific case of no curvature, $\gamma = \alpha = 0$, then $\tilde{f}''(0) = a_0(\mu)$ giving $f''(0) = A^{-1/2}a_0(\mu)$. In particular, there is a critical value $\mu_c = -1.4174$ giving

$$\lambda_c = -1.4174B^{-1} \quad (49)$$

showing that the values of $|\lambda_c|$ increase as the volume fraction of nanoparticles increase, thus giving a greater range of solutions in the opposing case. This expression is in agreement with the values for λ_c given in Fig. 2 on using the values of B given in Table 1. For the general case, for a given ϕ , first calculate $A = A(\phi)$ and $B = B(\phi)$ and hence calculate the modified curvature and mixed convection parameters α and μ from (46). Then, to find the critical values, for example, first determine the corresponding value of μ_c from Fig. 5 (say) and finally λ_c from (46). It is worth mentioning that rescaling analysis for the full problem might be done in a further study

6 Conclusions

We have considered the mixed convection boundary-layer flow and heat transfer on a vertical cylinder in a porous material filled with a nanofluid. We took specific forms for the outer flow and wall temperature variation that enabled the system to be reduced to similarity form, Eqs. (7–9) or Eqs. (13, 14). These equations involved the two parameters, $A(\phi)$ and $B(\phi)$, as defined in (10) and dependent on the nanoparticle volume fraction ϕ which characterized the particular nanoparticles and the fluid filling the porous material. Values of these parameters for Cu and water are given in Table 1. We used the physical properties for copper nanoparticles in water for our numerical calculations, though we expect the same general trends in behaviour for other similar fluids and types of nanoparticles.

We started by considering a pure fluid, Fig. 1, finding a critical value λ_c of the mixed convection parameter λ , with solutions existing only for $\lambda \geq \lambda_c$. We saw that the values of λ_c were negative, thus restrictions on the existence of a solution were confined to opposing flow, and that $|\lambda_c|$ increased as the curvature parameter γ was increased. This was confirmed in Fig. 5 where the behaviour of λ_c with γ is given for different volume fractions ϕ .

We then took specific values for the curvature parameter γ and plotted the skin friction $f''(0)$ and wall heat transfer $-\theta'(0)$ against λ for different nanoparticle volume fractions, see Figs. 2, 3, and 4. Our main conclusion was that adding nanoparticles to the base fluid decreases the skin friction and increases the wall heat transfer for aiding flow, $\lambda > 0$, whereas the opposite is the case for opposing flow, $\lambda_c \leq \lambda < 0$. These effect become more pronounced as the nanoparticle fraction ϕ is increased, for given values of the other parameters.

We then examined the free convection, $\lambda \rightarrow \infty$, limit finding that this was independent of curvature effects provided that γ was of $O(1)$. Our asymptotic results (23) for the skin friction and wall heat transfer confirmed those seen in our numerical results. We required γ to be large, specifically of $O(\lambda^{1/2})$, for curvature to have a significant effect, solutions to the resulting problem (27) are shown in Fig. 6. We then examined the effect that curvature have on the flow and heat transfer with plots of the skin friction $f''(0)$ against γ for $\lambda = 1.0$ given in Fig. 7a. We then obtained an asymptotic solution for large γ where we saw that the ultimate asymptotic limit is approached very slowly, the correction being of $O((\log \gamma)^{-1})$, as can be seen in Fig. 7b.

The understanding of the fundamentals of heat transfer and wall friction is prime importance for developing nanofluids for a wide range of heat transfer application. Although there are recent developments in the study of heat transfer with nanofluids, more experimental results and the theoretical understanding of the mechanisms of the particle movements are needed to understand heat transfer and fluid flow behaviour of nanofluids. Further work is also needed for the treatment of nanofluids as a two-phase flow since slip velocity between

the particle and base fluid plays important role on the heat transfer performance of nanofluids (Kakaç and Pramuanjaroenkij 2009).

Acknowledgments AMR and SA gratefully acknowledge the financial support received in the form of research grant: Fundamental Research Grant Scheme (203/PMATHS/6711234) from the Malaysia Ministry of Higher Education. AMR would like to acknowledge the financial support received from Universiti Utara Malaysia and Malaysia Ministry of Higher Education throughout the course of her study. We also would like to thank the reviewers for the valuable comments and suggestions

References

- Aly, E.H., Elliott, L., Ingham, D.B.: Mixed convection boundary-layer flow over a vertical surface embedded in a porous medium. *Eur. J. Mech. B Fluids* **22**, 529–543 (2003)
- Brinkman, H.C.: The viscosity of concentrated suspensions and solutions. *J. Chem. Phys.* **20**, 571–581 (1952)
- Buongiorno, J.: Convective transport in nanofluids. *ASME J. Heat Transf.* **128**, 240–250 (2006)
- Choi, S.U.S.: Enhancing thermal conductivity of fluids with nanoparticles. In: *Proceedings of the 1995 ASME International Mechanical Engineering Congress and Exposition, San Francisco, USA*. ASME, FED 231/MD, vol. 66, pp. 99–105 (1995)
- Das, S.K., Choi, S.U.S., Yu, W., Pradeep, T.: *Nanofluids: Science and Technology*. Wiley, Hoboken (2007)
- Eagen, J., Rusconi, R., Piazza, R., Yip, S.: The classical nature of thermal conduction in nanofluids. *ASME J. Heat Transfer* **132**, 102402 (14 pp) (2010)
- Fan, J., Wang, L.: Review of heat conduction in nanofluids. *ASME J. Heat Transfer* **133**, 040801 (14 pp) (2011)
- Ingham, D.B., Pop, I. (eds.): *Transport Phenomena in Porous Media*, vol. III. Elsevier, Oxford (2005)
- Kakaç, S., Pramuanjaroenkij, A.: Review of convective heat transfer enhancement with nanofluids. *Int. J. Heat Mass Transf.* **52**, 3187–3196 (2009)
- Khanafar, K., Vafai, K., Lightstone, M.: Buoyancy-driven heat transfer enhancement in a two-dimensional enclosure utilizing nanofluids. *Int. J. Heat Mass Transf.* **46**, 3639–3653 (2003)
- Kumar, S., Prasad, S.K., Banerjee, J.: Analysis of flow and thermal field in nanofluid using a single phase thermal dispersion model. *Appl. Math. Modell.* **34**, 573–592 (2010)
- Kuznetsov, A.V., Nield, D.A.: Thermal instability in a porous medium layer saturated by a nanofluid: Brinkman model. *Transp. Porous Media* **81**, 409–422 (2010a)
- Kuznetsov, A.V., Nield, D.A.: Effect of local thermal non-equilibrium on the onset of convection in a porous medium layer saturated by a nanofluid. *Transp. Porous Media* **83**, 425–436 (2010b)
- Kuznetsov, A.V., Nield, D.A.: The onset of double-diffusive nanofluid convection in a layer of a saturated porous medium. *Transp. Porous Media* **85**, 941–951 (2010c)
- Kuznetsov, A.V., Nield, D.A.: The Cheng–Minkowycz problem for the double-diffusive natural convective boundary layer flow in a porous medium saturated by a nanofluid. *Int. J. Heat Mass Transf.* **54**, 374–378 (2011a)
- Kuznetsov, A.V., Nield, D.A.: The effect of vertical throughflow on thermal instability in a porous medium layer saturated by a nanofluid. *Transp. Porous Media* **87**, 765–775 (2011b)
- Kuznetsov, A.V., Nield, D.A.: Double-diffusive natural convective boundary-layer flow of a nanofluid past a vertical plate. *Int. J. Therm. Sci.* **50**, 712–717 (2011c)
- Lee, J.H., Lee, S.H., Choi, C.J., Jang, S.P., Choi, S.U.S.: A review of thermal conductivity data, mechanics and models for nanofluids. *Int. J. Micro-Nano Scale Transp.* **1**, 269–322 (2010)
- Magyari, E.: Comment on the homogeneous nanofluid models applied to convective heat transfer problems. *Acta Mech.* **222**, 381–385 (2011a)
- Magyari, E.: Note on the “Scaling transformations for boundary layer flow near the stagnation-point on a heated permeable stretching surface in a porous medium saturated with a nanofluid and heat generation/absorption effects”. *Transp. Porous Media* **87**, 41–48 (2011b)
- Magyari, E.: Reply on the Reply on the “Note on the scaling transformations for boundary layer flow near the stagnation-point on a heated permeable stretching surface in a porous medium saturated with a nanofluid and heat generation/absorption effects”. *Transp. Porous Media* **87**, 53–56 (2011c)
- Magyari, E., Pop, I., Keller, B.: Exact solutions for a longitudinal steady mixed convection flow over a permeable vertical thin cylinder in a porous medium. *Int. J. Heat Mass Transf.* **48**, 3435–3442 (2003)
- Maliga, S.E.B., Palm, S.M., Nguyen, C.T., Roy, G., Galanis, N.: Heat transfer enhancement using nanofluid in forced convection flow. *Int. J. Heat Fluid Flow* **26**, 530–546 (2005)

- Mahmood, T., Merkin, J.H.: Similarity solutions in axisymmetric mixed-convection boundary-layer flow. *J. Eng. Math.* **22**, 73–92 (1988)
- Merkin, J.H.: Mixed convection boundary layer flow on a vertical surface in a saturated porous medium. *J. Eng. Math.* **14**, 301–313 (1980)
- Merkin, J.H.: On dual solutions occurring in mixed convection in a porous medium. *J. Eng. Math.* **20**, 171–179 (1985)
- Merkin, J.H., Mahmood, T.: Mixed convection boundary layer similarity solutions: prescribed wall heat flux. *J. Appl. Math. Phys. (ZAMP)* **40**, 51–68 (1989)
- Merkin, J.H., Pop, I.: Mixed convection boundary-layer on a vertical cylinder embedded in a saturated porous medium. *Acta Mech.* **66**, 251–262 (1987)
- Nield, D.A., Bejan, A.: *Convection in Porous Media*, 3rd edn. Springer, New York (2006)
- Nield, D.A., Kuznetsov, A.V.: The Cheng-Minkowycz problem for natural convective boundary-layer flow in a porous medium saturated by a nanofluid. *Int. J. Heat Mass Transf.* **52**, 5792–5795 (2009a)
- Nield, D.A., Kuznetsov, A.V.: Thermal instability in a porous medium layer saturated by a nanofluid. *Int. J. Heat Mass Transf.* **52**, 5796–5801 (2009b)
- Nield, D.A., Kuznetsov, A.V.: The onset of double-diffusive convection in a nanofluid layer. *Int. J. Heat Fluid Flow* **32**, 771–776 (2011)
- Oztop, H.F., Abu-Nada, E.: Numerical study of natural convection in partially heated rectangular enclosures filled with nanofluids. *Int. J. Heat Fluid Flow* **29**, 1326–1336 (2008)
- Pop, I.: Reply to the paper: Note on the “Scaling transformations for boundary layer flow near the stagnation-point on a heated permeable stretching surface in a porous medium saturated with a nanofluid and heat generation/absorption effects”. *Transp. Porous Media* **87**, 49–51 (2011)
- Pop, I., Ingham, D.B.: *Convective Heat Transfer: Mathematical and Computational Modeling of Viscous Fluids and Porous Media*. Pergamon, Oxford (2001)
- Sheikholeslami, M., Gorji-Bandpay, M., Ganji, D.D.: Magnetic field effects on natural convection around a horizontal circular cylinder inside a square enclosure filled with nanofluid. *Int. Commun. Heat Mass Transf.* **39**, 978–986 (2012a)
- Sheikholeslami, M., Ashorynejad, H.R., Domairry, G., Hashim, I.: Flow and heat transfer of Cu-water nanofluid between a stretching sheet and a porous surface in a rotating system. Hindawi Publishing Corporation. *J. Appl. Math.* Article ID 421320, 19 pp (2012b). doi:10.1155/2012/421320
- Soleimani, S., Sheikholeslami, M., Ganji, D.D., Gorji-Bandpay, M.: Natural convection heat transfer in a nanofluid filled semi-annulus enclosure. *Int. Commun. Heat Mass Transf.* **39**, 65–574 (2012)
- Tiwari, R.K., Das, M.K.: Heat transfer augmentation in a two-sided lid-driven differentially heated square cavity utilizing nanofluids. *Int. J. Heat Mass Transf.* **50**, 2002–2018 (2007)
- Trisaksri, V., Wongwises, S.: Critical review of heat transfer characteristics of nanofluids. *Renew. Sustain. Energy Rev.* **11**, 512–523 (2007)
- Vadasz, P.: *Emerging Topics in Heat and Mass Transfer in Porous Media*. Springer, New York (2008)
- Vafai, K. (ed.): *Handbook of Porous Media*, 2nd edn. Taylor and Francis, New York (2005)
- Vafai, K.: *Porous Media: Applications in Biological Systems and Biotechnology*. CRC Press, Tokyo (2010)
- Wong, K.F.V., Leon, O.D.: Applications of nanofluids: current and future. *Adv. Mech. Eng.* 519659 (11 pp) (2010)
- Wu, M., Kuznetsov, A.V., Jasper, W.J.: Modeling of particle trajectories in an electrostatically charged channel. *Phys. Fluids* **22**, 043301 (2010)
- Wu, G., Kuznetsov, A.V., Jasper, W.J.: Distribution characteristics of exhaust gases and soot particles in a wall-flow ceramics filter. *J. Aerosol. Sci.* **42**, 447–461 (2011)
- Xuan, Y., Roetzel, W.: Conceptions for heat transfer correlation of nanofluids. *Int. J. Heat Mass Transf.* **43**, 3701–3707 (2000)